HHS Public Access

Author manuscript

J Invest Dermatol. Author manuscript; available in PMC 2012 September 01.

Published in final edited form as:

J Invest Dermatol. 2012 March ; 132(3 0 1): 711–720. doi:10.1038/jid.2011.356.

CXCR4 Antagonist AMD3100 Accelerates Impaired Wound Healing in Diabetic Mice

Yukihide Nishimura, MD[1,2,3], **Masaaki Ii, MD, PhD**[1,4], **Gangjian Qin, MD**[1], **Hiromichi Hamada, MD, PhD**[5], **Jun Asai, MD, PhD**[2], **Hideya Takenaka, MD, PhD**[2], **Haruki Sekiguchi, MD, PhD**[1], **Marie-Ange Renault, PhD**[1], **Kentaro Jujo, MD, PhD**[1], **Norito Katoh, MD, PhD**[2], **Saburo Kishimoto, MD, PhD**[2], **Aiko Ito, PhD**[1], **Christine Kamide, BS**[1], **John Kenny, BS**[1], **Meredith Millay, BS**[1], **Sol Misener, AAS**[1], **Tina Thorne, MS**[1], and **Douglas W. Losordo, MD**[*,1]

[1]Feinberg Cardiovascular Research Institute, Northwestern University Feinberg School of Medicine, Chicago, IL, USA

[2]Department of Dermatology, Graduate School of Medical Science, Kyoto Prefectural University of Medicine, Kyoto, Japan

[3]Nishiyama Hospital, Nagaokakyo, Japan

[4] Department of Pharmacology, Osaka Medical College, Osaka, Japan

[5] Tokyo Women's Medical University, Yachiyo Medical Center, Chiba, Japan

Abstract

The antagonism of CXC-chemokine receptor 4 (CXCR4) with AMD3100 improves cardiac performance after myocardial infarction by augmenting the recruitment of endothelial progenitor cells (EPCs) from the bone marrow to the regenerating vasculature. We investigated whether AMD3100 may accelerate diabetes-impaired wound healing through a similar mechanism. Skin wounds were made on the backs of leptin-receptor–deficient mice and treated with AMD3100 or saline. Fourteen days after treatment, wound closure was significantly more complete in AMD3100-treated mice (AMD3100: 87.0±2.6%, Saline: 33.1±1.8%; P<0.0001) and was accompanied by greater collagen-fiber formation, capillary density, smooth-muscle-containing vessel density, and monocyte/macrophage infiltration. On day 7 after treatment, AMD3100 was associated with higher circulating EPC and macrophage counts and with significantly upregulated mRNA levels of stromal-cell–derived factor 1 and platelet-derived growth-factor B in the wound bed. AMD3100 also promoted macrophage proliferation and phagocytosis and the migration and proliferation of diabetic mouse primary dermal fibroblasts and 3T3 fibroblasts, which express very little CXCR4. In conclusion, a single topical application of AMD3100 promoted wound healing in diabetic mice by increasing cytokine production, mobilizing bone-marrow EPCs, and enhancing

[*]**Corresponding Author** Douglas W. Losordo, MD Feinberg Cardiovascular Research Institute Northwestern University Tarry 14-725 303 E. Chicago Ave. Chicago, IL 60611 Tel: 312-695-0072 Fax: 312-695-0047 d-losordo@northwestern.edu.

The work described in this manuscript was performed at the Feinberg Cardiovascular Research Institute, Northwestern University, Chicago, IL, USA

the activity of fibroblasts and monocytes/macrophages, thereby increasing both angiogenesis and vasculogenesis. Not all of the AMD3100-mediated effects evolved through CXCR4 antagonism.

Keywords

Diabetes; Angiogenesis; Wound healing

Introduction

Diabetes affects approximately 170 million people worldwide, including 20.8 million in the US, and these numbers are projected to double by 2030 (Brem and Tomic-Canic, 2007). In patients with diabetes, impaired angiogenesis and diminished granulation-tissue formation often couple with other factors, such as decreases in cell and growth-factor response, to reduce peripheral blood flow, which can retard wound healing and lead to the development of nonhealing foot ulcers (Brem and Tomic-Canic, 2007; Falanga, 2005; Jeffcoate and Harding, 2003). Non-healing ulcers affect 15% of people with diabetes and are a leading cause of amputation (Brem and Tomic-Canic, 2007; Falanga, 2005; Jeffcoate and Harding, 2003; Palumbo and Melton, 1995). Inflammation is a key component of the wound-healing response and mediates many of the effects induced by chemokines (Ochoa *et al.*, 2007) such as stromal-cell–derived factor 1 (SDF-1), which binds to CXC chemokine receptor 4 (CXCR4) and regulates both inflammation and cell migration (Rey *et al.*, 2007). Thus, interactions between SDF-1 and CXCR4 contribute to cutaneous wound healing (Avniel *et al.*, 2006), but the mechanisms involved remain incompletely characterized. Recent experiments conducted in our laboratory indicate that administration of the CXCR4 antagonist AMD3100 promotes neovascularization after myocardial infarction by mobilizing endothelial progenitor cells (EPCs) from the bone marrow and by enhancing EPC recruitment to the sites of ischemia (Jujo *et al.*, 2010). Here, we investigated whether AMD3100 promotes cutaneous wound healing through a similar mechanism.

Results

Topical AMD3100 accelerates wound healing in diabetic mice

Full thickness excisional skin wounds were created on the backs of db/db mice, treated with AMD3100 or saline, and examined 0, 7, and 14 days later (Figure 1A). On day 14, the extent of wound closure was significantly greater ($P<0.0001$) in mice treated with AMD3100 (86.97±2.55%) than in saline-treated mice (33.07±1.82%) (Figure 1B), and histological scores were significantly higher for AMD3100-treated wounds than for wounds treated with saline (Figures 1C-E) (epithelialization: AMD3100, 4.250±0.250, saline, 2.000±0.408, $P<0.005$; granulation: AMD3100, 4.750±0.479, saline, 2.250±0.479, $P<0.01$; inflammation: AMD3100, 3.750±0.250, saline, 2.500±0.289; $P<0.05$) (Figures 1C-E); inflammation scores were also significantly higher for AMD3100-treated wounds on day 7 (AMD3100, 3.500±0.289, saline, 1.500±0.289, $P<0.005$). Thick granulation tissue, extensive re-epithelialization, and persistent inflammation-related acanthosis were observed on the surface of AMD3100-treated wounds, and functional, erythrocyte-containing blood

vessels were prevalent in the deeper dermis, whereas saline-treated wounds exhibited a thin layer of granulation tissue and fewer functional blood vessels (Figure 1F).

AMD3100 enhances collagen formation at the wound site

Because collagen formation is a crucial component of wound healing, sections of wound tissue were stained to identify collagen in the granulation tissue (Masson's Trichrome staining) and to assess collagen-fiber formation at the wound center (picosirius red staining), which is the last region of the wound to heal. Fourteen days after wounding and treatment, collagen fibers were observed throughout the granulation tissue in AMD3100-treated wounds, but were restricted primarily to the edges of saline-treated wounds (Figure 2A). The collagen fibers in AMD3100-treated wounds were heterogeneous and appeared to contain a cellular (perhaps fibroblast) component, which suggests that the fibers were newly formed; AMD3100-treated wounds also displayed evidence of persistent acanthosis. At the wound center, collagen fibers were significantly more common ($P<0.05$) in AMD3100-treated wounds (9.210±1.883% of image area) than in wounds treated with saline (3.901±0.174% of image area) (Figure 2B).

AMD3100 increases capillary density, the formation of smooth muscle–containing vessels, and monocyte/macrophage infiltration

Fourteen days after wounding and treatment, capillary density was significantly higher ($P<0.01$) in AMD3100-treated wounds (3.81±0.54% of image area) than in wounds treated with saline (1.16±0.18% of image area) (Figure 2C, D), and smooth muscle–containing vessel-like structures were more common in the dermis of the AMD3100-treatment group (AMD3100: 52.2±8.0 vessels/high-power field [HPF], saline: 9.8±1.6 vessels/HPF; $P<0.001$) (Figure 2C, E). Cells stained positively for the monocyte/macrophage-specific marker CD68 (Figure 2F) were significantly more prevalent in wounds treated with AMD3100 than in saline-treated wounds on day 7 (AMD3100: 164.250±26.544 cells/HPF, saline: 28.750±5.735 cells/HPF; $P<0.01$) (Figure 2G), and real-time RT-PCR analyses of CD68 mRNA expression yielded similar results: treatment with AMD3100 was associated with significantly greater CD68 mRNA expression on day 7 (AMD3100: 230.163±18.913, saline: 69.912±8.638; $P<0.0001$) but not on day 14 (Figure 3A).

AMD3100 upregulates SDF-1α and platelet-derived growth factor B mRNA expression at the wound site

Real-time RT-PCR analyses of the expression of SDF-1α and platelet-derived growth factor (PDGF)-B, which are known to enhance progenitor-cell homing, indicated that both factors were expressed at significantly higher levels in wounds treated with AMD3100 than in saline-treated wounds on day 7 (SDF-1α: AMD3100, 107.160±24.067; saline, 28.533±1.639; $P<0.01$. PDGF-B: AMD3100, 5.427±0.626; saline, 2.840±0.319; $P<0.001$) but not on day 14 (Figure 3B, C).

AMD3100 mobilizes cells from the bone marrow to the peripheral circulation

To determine whether the accelerated healing observed after AMD3100 treatment was associated with enhanced mobilization of cells from the bone marrow, the number of EPCs

and macrophages in the peripheral blood was assessed 7 days after wounding and treatment. EPCs were identified by DiI-labeled acetylated low density lipoprotein (DiI-acLDL) uptake and Bandeiraea simplicifolia lectin 1(BS1-lectin) staining, whereas macrophages were identified via CD68 expression; isolectin B4 is a marker for macrophage activation (Guillemin and Brew, 2004; Maddox *et al.*, 1982; Sorokin and Hoyt, 1992; Warfel *et al.*, 1991), so cells stained positively for both isolectin B4 and CD68 expression were considered activated macrophages (Figure 4A). All three cell types were significantly more common (P<0.0001) in mice treated with AMD3100 (EPCs: 48.400±2.948 cells/HPF; macrophages: 27.600±0.909 cells/HPF, activated macrophages: 12.600±1.462 cells/HPF) than in the saline-treatment group (EPCs: 9.500±1.067 cells/HPF, macrophages: 7.000±0.816 cells/HPF, activated macrophages: 2.300±0.667 cells/HPF) (Figure 4B).

AMD3100 promotes the migration and proliferation of diabetic mouse primary dermal fibroblasts and the proliferative and phagocytosis activity of macrophages

The cellular mechanisms responsible for AMD3100-enhanced wound healing were investigated by evaluating the migration and proliferation of db/db mouse primary dermal fibroblasts in 5 mM and 25 mM D-glucose; measurements were repeated in 25 mM D-mannitol to serve as an osmotic control for the high-glucose condition. Fibroblasts migrated toward 2 μg/mL AMD3100 under all conditions (Figure 5A, B). In cells cultured at the high-glucose concentration, 2 μg/mL AMD3100 significantly promoted fibroblast proliferation (Figure 5C), but a higher AMD3100 concentration (10 μg/mL) was required to significantly stimulate proliferation under the low-glucose or osmotic-control conditions. AMD3100 also promoted the proliferation (2 μg/mL AMD3100: 0.307±0.013 OD, 0 μg/mL AMD3100: 0.191±0.007 OD; P<0.0001) and phagocytosis activity (2 μg/mL AMD3100: 0.487±0.019 OD, 0 μg/mL AMD3100: 0.351±0.019 OD; P<0.01) of macrophages, but did not significantly affect EPC proliferation (Figure 5D).

AMD3100 enhances fibroblast migration and proliferation in the absence of CXCR4 protein expression

AMD3100 is a CXCR4 antagonist, and CXCR4 is expressed in murine db/db fibroblasts; however, human fibroblasts do not express CXCR4 (Avniel *et al.*, 2006). Thus, we investigated whether CXCR4 is required for the AMD3100-induced enhancement of fibroblast migration and proliferation by performing experiments with NIH 3T3 fibroblasts, which express nearly undetectable amounts of CXCR4 mRNA (3T3: 0.001±0.0001, db/db: 0.047±0.005; P<0.0001). The migratory response of 3T3 fibroblasts was significantly enhanced by AMD3100 (2 μg/mL AMD3100: 250.267±18.032 cells/HPF, 0 μg/mL AMD3100: 112.167±17.559 cells/HPF; P<0.0001) (Figure 6A), and AMD3100 also promoted 3T3 fibroblast proliferation (2 μg/mL AMD3100: 0.337±0.015 OD, 0 μg/mL AMD3100: 0.256±0.008 OD; P<0.001) (Figure 6B). To characterize the molecular mechanisms responsible for the AMD3100-induced enhancement of 3T3 fibroblast activity, we measured the mRNA expression of a panel of candidate factors. After 12 hours in culture, treatment with AMD3100 was associated with significant upregulation of SDF-1α (2 μg/mL AMD3100: 104.594±2.234, 0 μg/mL AMD3100: 70.058±4.105; P<0.0001), PDGF-B (2 μg/mL AMD3100: 0.045±0.001, 0 μg/mL AMD3100: 0.014±0.003; P<0.0001),

and MCP-1 (2 μg/mL AMD3100: 12.528±1.819, 0 μg/mL AMD3100: 6.645±2.121; $P<0.05$) mRNA expression (Figure 6C).

Discussion

Therapeutic strategies that block the interaction between CXCR4 and SDF-1 are promising treatments for a variety of clinical applications. CXCR4 was first identified as a co-receptor for cellular entry of the human immunodefficiency virus (HIV) (Bleul *et al.*, 1996), and more recent evidence indicates that CXCR4 has a role in stem-cell trafficking, vascular growth, and cancer metastasis (Orimo *et al.*, 2005; Petit *et al.*, 2002; Staller *et al.*, 2003; Urbich and Dimmeler, 2004; Yamaguchi *et al.*, 2003). AMD3100 was the first CXCR4 antagonist to enter clinical trials, and although it failed as an anti-HIV drug, phase 3 trials for its use in stem-cell mobilization have recently been completed (Adis Data Information BV, 2007).

Angiogenesis is a crucial component of wound healing (Brem and Tomic-Canic, 2007; Falanga, 2005; Singer and Clark, 1999); however, peripheral blood flow is often impaired in patients with diabetes, which can retard wound healing and lead to the development of nonhealing ulcers and subsequent amputation (Brem and Tomic-Canic, 2007; Falanga, 2005; Jeffcoate and Harding, 2003; Palumbo and Melton, 1995). Current treatments for nonhealing ulcers often combine off-loading (Boulton *et al.*, 2005) with the administration of growth factors (e.g., PDGF-BB (Smiell, 1998)) and/or cell-based approaches delivered in an absorbable mesh (fibroblasts) (Marston *et al.*, 2003) or in type 1 collagen (fibroblasts and keratinocytes) (Brem *et al.*, 2000). Here, we investigated whether the angiogenic effects associated with AMD3100 administration could improve cutaneous wound healing in genetically diabetic mice, which, like patients with diabetes, display impairments in wound healing, granulation tissue formation, and angiogenesis (Greenhalgh *et al.*, 1990; Werner *et al.*, 2007). However, mouse models of chronic wound repair do not always replicate the human experience, so our findings must be interpreted with caution.

Our results indicate that topical application of AMD3100 accelerates wound healing in diabetic mice. Wound closure was 2.5-fold more complete 14 days after treatment with AMD3100 than after saline treatment and was accompanied by significantly higher histological scores, notably thicker granulation tissue (perhaps associated with acanthosis), and improved collagen deposition and fiber formation. AMD3100 treatment was also associated with greater macrophage accumulation and PDGF-B expression at the wound site. Because PDGF-B promotes macrophage activation, fibroblast proliferation, and the recruitment of both cell types (Singer and Clark, 1999), topical AMD3100 treatment likely enhances wound healing by inducing a variety of effects in both macrophages and fibroblasts. However, not all of these effects can be attributed to CXCR4 antagonism, because AMD3100 stimulated the migration and proliferation of 3T3 fibroblasts, which express little, if any, CXCR4.

Capillaries and smooth muscle–containing vessels were more prevalent in AMD3100-treated wounds than in wounds treated with saline, suggesting that AMD3100 promotes neovascularization (i.e., the development of new blood vessels) and vascular remodeling

(i.e., arteriogenesis). Neovascularization occurs via two processes: angiogenesis, the proliferation and migration of pre-existing, fully-differentiated endothelial cells in nearby vessels; and vasculogenesis, the *de-novo* assembly of new blood vessels (Folkman and Shing, 1992; Isner and Asahara, 1999). Historically, vasculogenesis was believed to occur only during embryogenesis; however, the results from more recent experiments indicate that EPCs in the peripheral blood participate in postnatal vasculogenesis by incorporating into new vessels and by expressing a variety of growth factors in ischemic tissue (Asahara *et al.*, 1997; Isner and Asahara, 1999; Jujo *et al.*, 2010; Velazquez, 2007). In the absence of ischemia, interactions between CXCR4 and SDF-1α sequester EPCs in the bone marrow, but disruption of the SDF-1α/CXCR4 axis with AMD3100 mobilizes these (and other) cells to the peripheral circulation (Broxmeyer *et al.*, 2005; Shepherd *et al.*, 2006), as evidenced by the elevated peripheral-blood EPC and macrophage counts observed in mice treated with topical AMD3100.

In both patients and animal models, diabetes is associated with low circulating EPC counts (Capla *et al.*, 2007; Chen *et al.*, 2007; Gallagher *et al.*, 2007; Schatteman and Ma, 2006; Tepper *et al.*, 2002; Vasa *et al.*, 2001) and a loss of SDF-1α expression in ischemic tissue, which impairs the recruitment of circulating EPCs to the injury site (Brem and Tomic-Canic, 2007; Gallagher *et al.*, 2007). Impaired EPC recruitment in genetically diabetic mice (Gallagher *et al.*, 2007), streptozotocin-induced diabetic mice (Sivan-Loukianova *et al.*, 2003), and in nude mice (Suh *et al.*, 2005) can be circumvented by administering human EPCs directly to the cutaneous wound, and both EPC mobilization and recruitment can be enhanced by topical application of SDF-1α to the wounds of db/db mice (Gallagher *et al.*, 2007). Here, we demonstrated that topical AMD3100 increases both peripheral-blood EPC counts and the expression of SDF-1α at the wound site, so the improved neovascularization and wound healing associated with AMD3100 treatment likely evolved, at least in part, via enhanced EPC recruitment. Topical application of VEGF (Galiano *et al.*, 2004), sonic hedgehog (Asai *et al.*, 2006b), or dibutyryl cAMP (Asai *et al.*, 2006a) to cutaneous wounds has also been shown to increase neovascularization by increasing EPC mobilization and/or recruitment.

Dermal fibroblasts are among the primary targets of PDGF during cutaneous wound healing (Singer and Clark, 1999). The two PDGF receptor (PDGFR) subtypes, PDGFR-α and PDGFR-β, have distinct roles in development, and PDGFR-β is an important mediator for the contribution of dermal fibroblasts to wound healing (Gao *et al.*, 2005). The role of the PDGF-B/PDGFR-β system in adult tissues has been difficult to characterize, because homozygous disruption of either PDGF-B or PDGFR-β in mice results in perinatal death (Gao *et al.*, 2005); however, blockade of PDGF-BB signaling delays tumor growth (Bergers *et al.*, 2003) and cutaneous wound healing (Rajkumar *et al.*, 2006). Collectively, these observations suggest that AMD3100 accelerates wound healing primarily by increasing fibroblast activity and noevascularization, although enhancements in keratinocyte activity and re-epithelialization cannot be excluded.

In conclusion, the results from our investigation indicate that a single topical application of AMD3100 promotes cutaneous wound healing and neovascularization in diabetic mice, and that these effects are likely induced both directly, through enhanced fibroblast and

macrophage activity, and indirectly, through the stimulation of cytokine production and the mobilization of progenitor cells from the bone marrow into the peripheral circulation. Our findings must be interpretted with caution, however, because the results from mouse models of chronic wound repair do not always predict patient response. Future investigations are warranted to determine the potential clinical utility of this compound for the treatment of nonhealing skin ulcers in patients with diabetes or microvascular disorders.

Materials and Methods

Animals, wound model, and treatment

The Institutional Animal Care and Use Committee of Northwestern University approved all described studies. Experiments were performed with 10- to 12-week-old female, genetically diabetic, C57BLKS/J-m$^{+/+}$ *Lepr*^{db} (db/db) mice and their C57BLKS/6J wild-type littermates (The Jackson Laboratories, Bar Harbor, ME, USA). Cutaneous wounds were created as described previously (Asai *et al.*, 2006a; Asai *et al.*, 2006b; Greenhalgh *et al.*, 1990; Maruyama *et al.*, 2007) and as summarized in the Supplemental Methods. Immediately after wounding, 6 mg/kg AMD3100 octahydrochloride (Sigma-Aldrich Co., St. Louis, MO, USA) in 30 μL saline or saline alone was topically applied to the wound bed, and then a semipermeable transparent dressing was placed over the wound, secured to the surrounding skin and muscle with 6-0 Prolene surtures, and left in place until subsequent evaluations were performed (i.e., for up to 14 days after wounding); suture use was minimized and did not interfere with wound contraction. The AMD3100 dose was determined in preliminary experiments: 2-, 6-, and 10-mg doses were tested, and the 6-mg dose was the minimum required to achieve the greatest acceleration of wound healing.

Wound closure

Wounds were photographed with a digital camera (Nikon Coolpix 995; Nikon Inc., Melville, NY, USA), then images were analyzed by tracing the wound margin with a fine-resolution computer mouse and calculating the enclosed pixel area with National Institute of Health (NIH) Image software (Asai *et al.*, 2006a; Asai *et al.*, 2006b; Greenhalgh *et al.*, 1990; Maruyama *et al.*, 2007). Measurements were performed in duplicate, and the percentage of wound closure was calculated by using the following equation:

$$\text{Wound closure}\,(\%) = \frac{\text{Wound area on day } 0 - \text{Wound area on the indicated day}}{\text{Wound area on day } 0} \times 100\%$$

Histological scores

Wound tissue was harvested, fixed in 100% methanol, processed by standard methods, and cut into 5-μm sections; then, the sections were paraffin-embedded, stained with hematoxylin and eosin, and viewed with an Olympus VANOX AHBT3 (Olympus America Inc, Center Valley, PA, USA). Epithelialization, granulation, and inflammation were rated from 1 (little or none) to 5 (extensive or severe) by investigators who were blind to treatment as described previously (Asai *et al.*, 2006a; Asai *et al.*, 2006b; Greenhalgh *et al.*, 1990; Maruyama *et al.*, 2007) with modifications.

Collagen formation

Collagen formation was evaluated as described previously (Asai *et al.*, 2006a; Asai *et al.*, 2006b) in 5-μm, paraffin-embedded sections of wound tissue that were stained with Masson trichrome. To evaluate collagen fiber formation at the wound center, sections were stained with picosirius red and viewed under polarized light to accentuate the birefringence of collagen fibers (Junqueira *et al.*, 1979). Fiber formation was quantified as the percentage of the digitized image that fluoresced red (mature fibers) or yellow-green (immature fibers).

Wound vascularity

Vasculature in the healing wound was evaluated as described previously (Asai *et al.*, 2006a; Asai *et al.*, 2006b). Wounds were harvested, sectioned, and then stained with fluorescein isothiocyanate (FITC)–conjugated BS-1 lectin and with mouse monoclonal alkaline-phosphatase anti-smooth-muscle α-actin (αSMA) (1:100) (Sigma-Aldrich Co.). Nuclei were counterstained with 4',6-diamidino-2-phenylindole (DAPI). The sections were viewed with a Carl Zeiss Axio Observer.D1 (Carl Zeiss MicroImaging Inc, Thornwood, NY, USA) (50× magnification) and digitally photographed. Capillary density was quantified as the percentage of the image area that fluoresced positively for FITC-BS1 lectin, and smooth muscle–containing vessels were identified by positive staining for both FITC-BS1 lectin and αSMA. Assessments were performed in 3 sections, 4 HPFs per section.

Infiltration of monocytes/macrophages

Paraffin-embedded, 5-μm sections of wound tissue were sequentially stained with rat monoclonal anti-mouse CD68 primary antibodies (AbD Serotec, Raleigh, NC, USA) and Alexa Fluor 555 goat anti-rat IgG secondary antibodies (Invitrogen Corporation, Carlsbad, CA, USA). Secondary staining with normal rat IgG was performed as a negative control, and nuclei were counterstained with DAPI. Sections were viewed with a Carl Zeiss Axio Observer.D1 and Image J™ software (NIH, USA) (to enable adjustment of the threshold of fluorescence intensity); cells located at the wound center and stained positively for CD68 expression were counted in 3 sections, 4 HPFs per section.

Mobilization of bone marrow–derived cells

Circulating EPC levels were evaluated as described previously (Iwakura *et al.*, 2003). Mononuclear cells were isolated from 500 μL of peripheral blood via gradient centrifugation with Histopaque-1083 (Sigma-Aldrich Co.); then, cells were seeded on 4-well chamber slides, coated with rat vitronectin, and cultured in 5% fetal bovine serum (FBS)/EBM-2 medium supplemented with growth factors (SingleQuot Kit; Clonetics Corp., San Diego, CA, USA). After 4 days in culture, cells were incubated with DiI-acLDL (Biomedical Technologies, Inc., Stoughton, MA, USA) for 1 hour and stained with FITC-conjugated BS-1 lectin (Vector Laboratories, Burlingame, CA, USA), and then the slides were viewed with a Carl Zeiss Axio Observer.D1 and Image J™ software (NIH, USA). Double-stained cells were considered EPCs and counted in 3 wells, 10 randomly selected HPFs per well.

To determine the number of monocytes/macrophages present in the peripheral circulation, mononuclear cells were isolated from 500 μL of peripheral blood via a gradient

centrifugation, seeded on 4-well chamber slides, and cultured in RPMI 1640 medium containing 10% heat-inactivated FBS. After 4 days in culture, cells were sequentially incubated with anti-CD68 antibodies (AbD Serotec), Alexa Fluor 555 goat anti-rat IgG secondary antibodies (Invitrogen Corporation), and FITC-conjugated isolectin B4 (Vector Laboratories), and then the slides were viewed with a Carl Zeiss Axio Observer.D1 and Image J™ software (NIH, USA). Cells stained positively for CD68 expression were considered macrophages, and cells stained positively for both CD68 and isolectin B4 were considered activated macrophages; the identified cells were counted in 3 wells, 10 HPFs per well.

Additional cell populations

Primary isolates of dermal fibroblasts, bone marrow–derived macrophages, and 3T3 fibroblasts were obtained and cultured as summarized in the Supplemental Methods.

Cell functional assays

Migration was evaluated via a modified Boyden's chamber assay, proliferation was evaluated via the CellTiter 96 nonradioactive cell proliferation assay (Promega Corporation, Madison, WI, USA), and phagocytosis was evaluated via the CytoSelect™ 96-well phagocytosis assay (red blood cell, colorimetric format; Cell Biolabs, Inc., San Diego, CA, USA) as directed by the manufacturer's instructions. The protocols are summarized in the Supplemental Methods.

Quantitative real-time reverse-transcriptase polymerase chain reaction (qRT-PCR)

Quantitative RT-PCR analyses were performed via standardized protocols as summarized in the Supplemental Methods and normalized to endogenous 18S rRNA expression. Primer and probe sequences are listed in Table S1.

Statistical analyses

All results are presented as mean ± SEM. Comparisons between 2 groups were evaluated with the Student's *t*-test, and comparisons among 3 or more groups were evaluated via one-way ANOVA followed by post-hoc testing with the Tukey procedure. A *P* value of less than 0.05 was considered statistically significant.

Supplementary Material

Refer to Web version on PubMed Central for supplementary material.

Acknowledgments

We thank K. Krueger for administrative assistance, W. Kevin Meisner, Ph.D., ELS, for editorial support, and Dr. Christopher H. Fung for assistance with our histological assessments.

Conflict of Interest

This study was supported in part by grants from the NIH (HL-53354, HL-77428, HL-63414, HL-80137, HL95874, HLPO1-66957 and HL-57516) and Eli Lilly Japan K.K. Foundation. The authors declare no conflict of interest.

Abbreviations

BS1-lectin	Bandeiraea simplicifolia lectin 1
CXCR4	CXC-chemokine receptor 4
DAPI	4',6-diamidino-2-phenylindole
DiI-acLDL	DiI-labeled acetylated low density lipoprotein
EPC	endothelial progenitor cell
HPF	high-power field
PDGF	platelet-derived growth factor
PDGFR	platelet-derived growth-factor receptor
SDF-1	stromal-cell-derived factor 1
αSMA	smooth-muscle α-actin

References

Adis Data Information BV. Plerixafor: AMD 3100, AMD3100, JM 3100, SDZ SID 791. Drugs R D. 2007; 8:113–119. [PubMed: 17324009]

Asahara T, Murohara T, Sullivan A, et al. Isolation of putative progenitor endothelial cells for angiogenesis. Science. 1997; 275:964–967. [PubMed: 9020076]

Asai J, Takenaka H, Katoh N, et al. Dibutyryl cAMP influences endothelial progenitor cell recruitment during wound neovascularization. J Invest Dermatol. 2006a; 126:1159–1167. [PubMed: 16514413]

Asai J, Takenaka H, Kusano KF, et al. Topical sonic hedgehog gene therapy accelerates wound healing in diabetes by enhancing endothelial progenitor cell-mediated microvascular remodeling. Circulation. 2006b; 113:2413–2424. [PubMed: 16702471]

Avniel S, Arik Z, Maly A, et al. Involvement of the CXCL12/CXCR4 pathway in the recovery of skin following burns. J Invest Dermatol. 2006; 126:468–476. [PubMed: 16385346]

Bergers G, Song S, Meyer-Morse N, et al. Benefits of targeting both pericytes and endothelial cells in the tumor vasculature with kinase inhibitors. J Clin Invest. 2003; 111:1287–1295. [PubMed: 12727920]

Bleul CC, Farzan M, Choe H, et al. The lymphocyte chemoattractant SDF-1 is a ligand for LESTR/fusin and blocks HIV-1 entry. Nature. 1996; 382:829–833. [PubMed: 8752280]

Boulton AJ, Vileikyte L, Ragnarson-Tennvall G, et al. The global burden of diabetic foot disease. Lancet. 2005; 366:1719–1724. [PubMed: 16291066]

Brem H, Balledux J, Bloom T, et al. Healing of diabetic foot ulcers and pressure ulcers with human skin equivalent: a new paradigm in wound healing. Arch Surg. 2000; 135:627–634. [PubMed: 10843357]

Brem H, Tomic-Canic M. Cellular and molecular basis of wound healing in diabetes. J Clin Invest. 2007; 117:1219–1222. [PubMed: 17476353]

Broxmeyer HE, Orschell CM, Clapp DW, et al. Rapid mobilization of murine and human hematopoietic stem and progenitor cells with AMD3100, a CXCR4 antagonist. J Exp Med. 2005; 201:1307–1318. [PubMed: 15837815]

Capla JM, Grogan RH, Callaghan MJ, et al. Diabetes impairs endothelial progenitor cell-mediated blood vessel formation in response to hypoxia. Plast Reconstr Surg. 2007; 119:59–70. [PubMed: 17255657]

Chen YH, Lin SJ, Lin FY, et al. High glucose impairs early and late endothelial progenitor cells by modifying nitric oxide-related but not oxidative stress-mediated mechanisms. Diabetes. 2007; 56:1559–1568. [PubMed: 17389326]

Falanga V. Wound healing and its impairment in the diabetic foot. Lancet. 2005; 366:1736–1743. [PubMed: 16291068]

Folkman J, Shing Y. Angiogenesis. J Biol Chem. 1992; 267:10931–10934. [PubMed: 1375931]

Galiano RD, Tepper OM, Pelo CR, et al. Topical vascular endothelial growth factor accelerates diabetic wound healing through increased angiogenesis and by mobilizing and recruiting bone marrow-derived cells. Am J Pathol. 2004; 164:1935–1947. [PubMed: 15161630]

Gallagher KA, Liu ZJ, Xiao M, et al. Diabetic impairments in NO-mediated endothelial progenitor cell mobilization and homing are reversed by hyperoxia and SDF-1 alpha. J Clin Invest. 2007; 117:1249–1259. [PubMed: 17476357]

Gao Z, Sasaoka T, Fujimori T, et al. Deletion of the PDGFR-beta gene affects key fibroblast functions important for wound healing. J Biol Chem. 2005; 280:9375–9389. [PubMed: 15590688]

Greenhalgh DG, Sprugel KH, Murray MJ, et al. PDGF and FGF stimulate wound healing in the genetically diabetic mouse. Am J Pathol. 1990; 136:1235–1246. [PubMed: 2356856]

Guillemin GJ, Brew BJ. Microglia, macrophages, perivascular macrophages, and pericytes: a review of function and identification. J Leukoc Biol. 2004; 75:388–397. [PubMed: 14612429]

Isner JM, Asahara T. Angiogenesis and vasculogenesis as therapeutic strategies for postnatal neovascularization. J Clin Invest. 1999; 103:1231–1236. [PubMed: 10225965]

Iwakura A, Luedemann C, Shastry S, et al. Estrogen-mediated, endothelial nitric oxide synthase-dependent mobilization of bone marrow-derived endothelial progenitor cells contributes to reendothelialization after arterial injury. Circulation. 2003; 108:3115–3121. [PubMed: 14676142]

Jeffcoate WJ, Harding KG. Diabetic foot ulcers. Lancet. 2003; 361:1545–1551. [PubMed: 12737879]

Jujo K, Hamada H, Iwakura A, et al. CXCR4 blockade augments bone marrow progenitor cell recruitment to the neovasculature and reduces mortality after myocardial infarction. Proc Natl Acad Sci U S A. 2010

Junqueira LC, Bignolas G, Brentani RR. Picrosirius staining plus polarization microscopy, a specific method for collagen detection in tissue sections. Histochem J. 1979; 11:447–455. [PubMed: 91593]

Maddox DE, Shibata S, Goldstein IJ. Stimulated macrophages express a new glycoprotein receptor reactive with Griffonia simplicifolia I-B4 isolectin. Proc Natl Acad Sci U S A. 1982; 79:166–170. [PubMed: 6798567]

Marston WA, Hanft J, Norwood P, et al. The efficacy and safety of Dermagraft in improving the healing of chronic diabetic foot ulcers: results of a prospective randomized trial. Diabetes Care. 2003; 26:1701–1705. [PubMed: 12766097]

Maruyama K, Asai J, Ii M, et al. Decreased macrophage number and activation lead to reduced lymphatic vessel formation and contribute to impaired diabetic wound healing. Am J Pathol. 2007; 170:1178–1191. [PubMed: 17392158]

Ochoa O, Torres FM, Shireman PK. Chemokines and diabetic wound healing. Vascular. 2007; 15:350–355. [PubMed: 18053419]

Orimo A, Gupta PB, Sgroi DC, et al. Stromal fibroblasts present in invasive human breast carcinomas promote tumor growth and angiogenesis through elevated SDF-1/CXCL12 secretion. Cell. 2005; 121:335–348. [PubMed: 15882617]

Palumbo, PJ.; Melton, JL, III. Peripheral vascular disease and diabetes.. In: Harris, MI.; Cowie, CC.; Stern, MP.; Boyko, EJ.; Reiber, GE.; Bennett, PH., editors. Diabetes in America. National Institute of Diabetes and Digestive and Kidney Diseases; Washington: 1995. p. 401-408.

Petit I, Szyper-Kravitz M, Nagler A, et al. G-CSF induces stem cell mobilization by decreasing bone marrow SDF-1 and up-regulating CXCR4. Nat Immunol. 2002; 3:687–694. [PubMed: 12068293]

Rajkumar VS, Shiwen X, Bostrom M, et al. Platelet-derived growth factor-beta receptor activation is essential for fibroblast and pericyte recruitment during cutaneous wound healing. Am J Pathol. 2006; 169:2254–2265. [PubMed: 17148686]

Rey M, Valenzuela-Fernandez A, Urzainqui A, et al. Myosin IIA is involved in the endocytosis of CXCR4 induced by SDF-1alpha. J Cell Sci. 2007; 120:1126–1133. [PubMed: 17327270]

Schatteman GC, Ma N. Old bone marrow cells inhibit skin wound vascularization. Stem Cells. 2006; 24:717–721. [PubMed: 16269529]

Shepherd RM, Capoccia BJ, Devine SM, et al. Angiogenic cells can be rapidly mobilized and efficiently harvested from the blood following treatment with AMD3100. Blood. 2006; 108:3662–3667. [PubMed: 16912220]

Singer AJ, Clark RA. Cutaneous wound healing. N Engl J Med. 1999; 341:738–746. [PubMed: 10471461]

Sivan-Loukianova E, Awad OA, Stepanovic V, et al. CD34+ blood cells accelerate vascularization and healing of diabetic mouse skin wounds. J Vasc Res. 2003; 40:368–377. [PubMed: 12891006]

Smiell JM. Clinical safety of becaplermin (rhPDGF-BB) gel. Becaplermin Studies Group. Am J Surg. 1998; 176:68S–73S. [PubMed: 9777975]

Sorokin SP, Hoyt RF Jr. Macrophage development: I. Rationale for using Griffonia simplicifolia isolectin B4 as a marker for the line. Anat Rec. 1992; 232:520–526. [PubMed: 1372795]

Staller P, Sulitkova J, Lisztwan J, et al. Chemokine receptor CXCR4 downregulated by von Hippel-Lindau tumour suppressor pVHL. Nature. 2003; 425:307–311. [PubMed: 13679920]

Suh W, Kim KL, Kim JM, et al. Transplantation of endothelial progenitor cells accelerates dermal wound healing with increased recruitment of monocytes/macrophages and neovascularization. Stem Cells. 2005; 23:1571–1578. [PubMed: 16081667]

Tepper OM, Galiano RD, Capla JM, et al. Human endothelial progenitor cells from type II diabetics exhibit impaired proliferation, adhesion, and incorporation into vascular structures. Circulation. 2002; 106:2781–2786. [PubMed: 12451003]

Urbich C, Dimmeler S. Endothelial progenitor cells: characterization and role in vascular biology. Circ Res. 2004; 95:343–353. [PubMed: 15321944]

Vasa M, Fichtlscherer S, Aicher A, et al. Number and migratory activity of circulating endothelial progenitor cells inversely correlate with risk factors for coronary artery disease. Circ Res. 2001; 89:E1–E7. [PubMed: 11440984]

Velazquez OC. Angiogenesis and vasculogenesis: inducing the growth of new blood vessels and wound healing by stimulation of bone marrow-derived progenitor cell mobilization and homing. J Vasc Surg. 2007; 45(Suppl A):A39–47. [PubMed: 17544023]

Warfel AH, Zucker-Franklin D, Zheng ZY. Macrophage membrane glycoproteins that bind Griffonia simplicifolia I-B4: effect on cytotoxicity and protein secretion. J Cell Physiol. 1991; 147:265–273. [PubMed: 1710228]

Werner C, Kamani CH, Gensch C, et al. The peroxisome proliferator-activated receptor-gamma agonist pioglitazone increases number and function of endothelial progenitor cells in patients with coronary artery disease and normal glucose tolerance. Diabetes. 2007; 56:2609–2615. [PubMed: 17623816]

Yamaguchi J, Kusano KF, Masuo O, et al. Stromal cell-derived factor-1 effects on ex vivo expanded endothelial progenitor cell recruitment for ischemic neovascularization. Circulation. 2003; 107:1322–1328. [PubMed: 12628955]

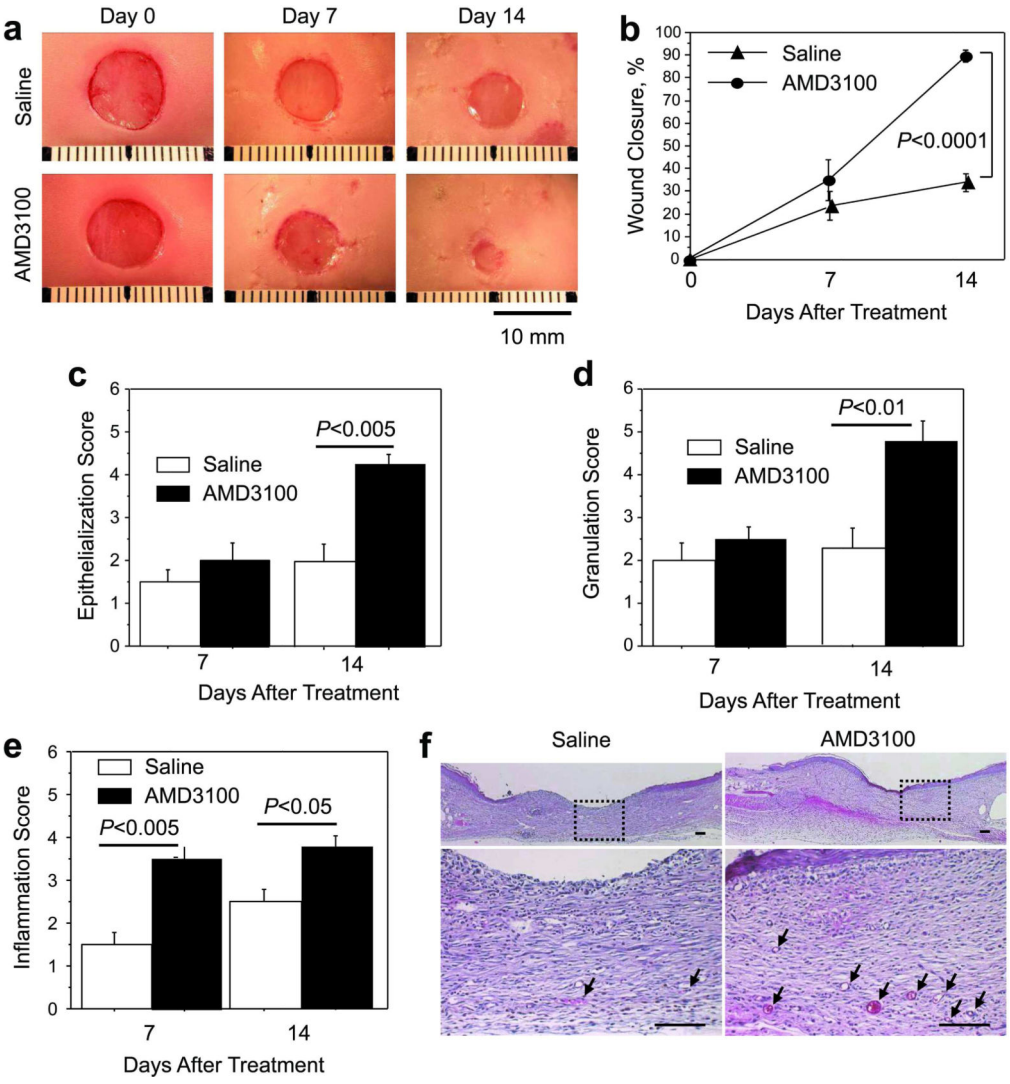

Figure 1. Wound-healing in diabetic mice

Full-thickness, excisional skin wounds were created on the backs of genetically diabetic (leptin receptor–deficient) mice, treated with 6 mg/kg AMD3100 in 30 μL saline or saline alone, then examined 0, 7, and 14 days later. (**A**) Wounds were digitally photographed, and (**B**) the extent of wound closure was expressed as the percentage decline in wound area. (**C**) Epithelialization, (**D**) granulation, and (**E**) inflammation scores ranging from 1 (little or none) to 5 (extensive or severe) were assigned to sections of hematoxylin and eosin–stained wound tissue harvested 14 days after treatment. Scores were summarized as the mean±SEM for each treatment group. (**F**) Representative sections of wound tissue harvested 14 days after treatment; the boxed regions in the upper panels (50× magnification) are displayed at higher magnification (200× magnification) in the lower panels. Functional blood vessels are identified with arrows. Bar=100 μm.

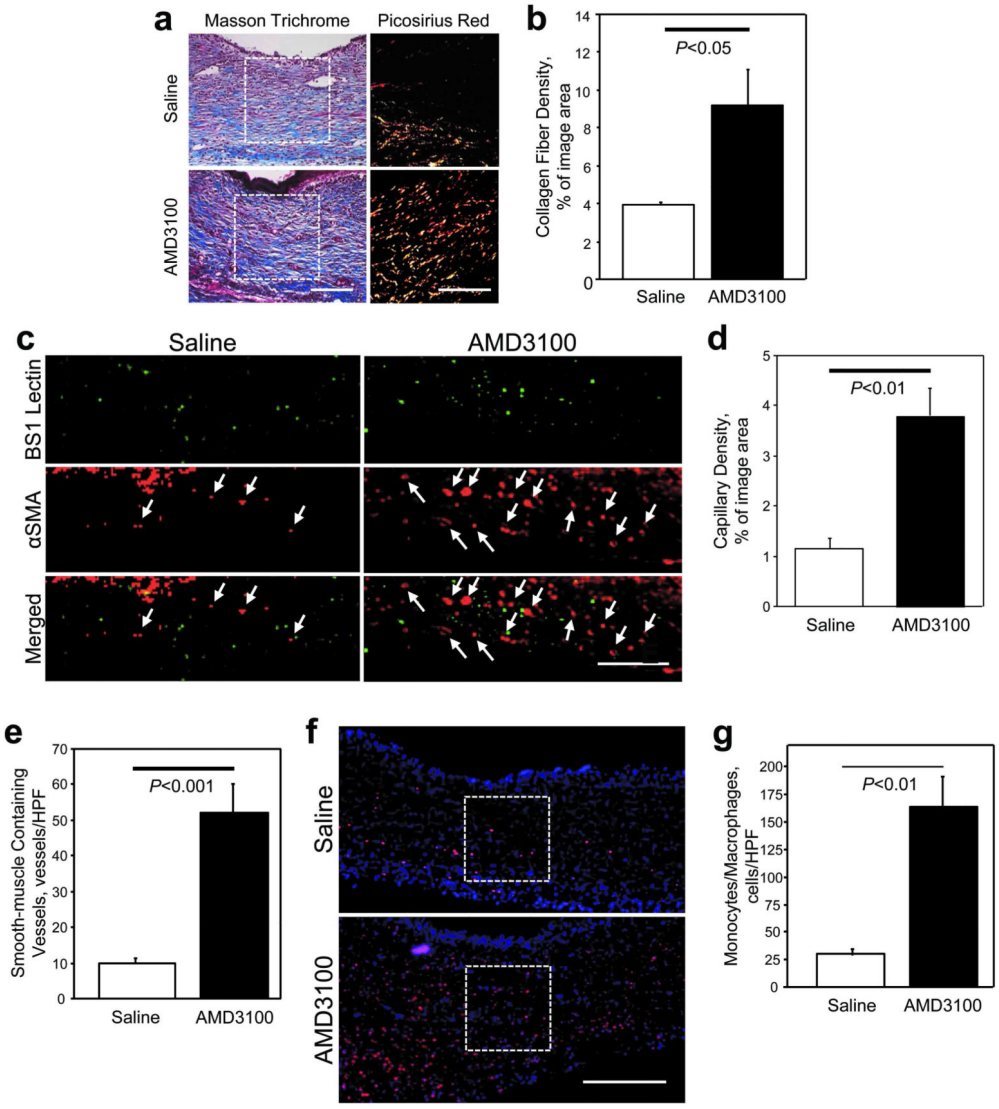

Figure 2. Collagen formation, vascularity, and monocyte/macrophage infiltration at the wound site

Collagen formation, vascularity, and monocyte/macrophage infiltration were evaluated 14 days, 14 days, and 7 days, respectively, after wounds were treated with 6 mg/kg AMD3100 in 30 μL saline or saline alone. (**A, B**) Collagen formation was assessed in sections of wound tissue stained with Masson trichrome or picrosirius red; picosirius red stain accentuates the birefringence of collagen fibers when viewed under polarized light. The boxed regions in the Masson-trichrome–stained panels (left) are displayed with picrosirius red staining in the right panels. Bar=100 μm. (**B**) Fiber formation at the wound center was quantified as the percentage of the digitized image area that fluoresced red (mature fibers) or yellow-green (immature fibers). (**C**) Wound tissue sections were stained with FITC-conjugated BS1 lectin (green) to identify endothelial tissue and with alkaline-phosphatase αSMA (red) to identify smooth-muscle cells. αSMA-positive vessels are identified with arrows. Bar=100 μm. (**D**) Capillary density was quantified as the percentage of the image area that fluoresced positively for BS1 lectin, and (**E**) smooth muscle–containing vessels were quantified as the

number of structures in the dermis that stained positively for both BS1 lectin and αSMA. (**F**) Sections of wound tissue were stained for expression of the monocyte/macrophage marker CD68 (red); nuclei were counterstained with DAPI (blue); bar=100 μm. The boxed regions were evaluated for quantification of (**G**) monocyte/macrophage infiltration (i.e., the number of CD68-positive cells).

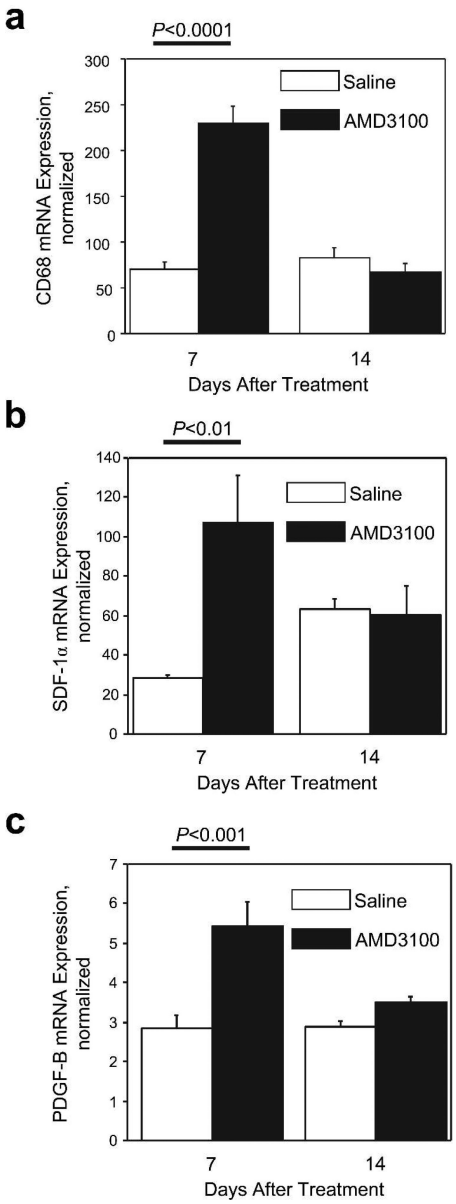

Figure 3. mRNA expression at the wound site

The expression of (**A**) CD68, (**B**) SDF-1α, and (**C**) PDGF-B in wound tissues was assessed 7 and 14 days after wounds were treated with 6 mg/kg AMD3100 in 30 μL saline or saline alone; measurements were performed via quantitative real-time RT-PCR and normalized to 18S rRNA expression.

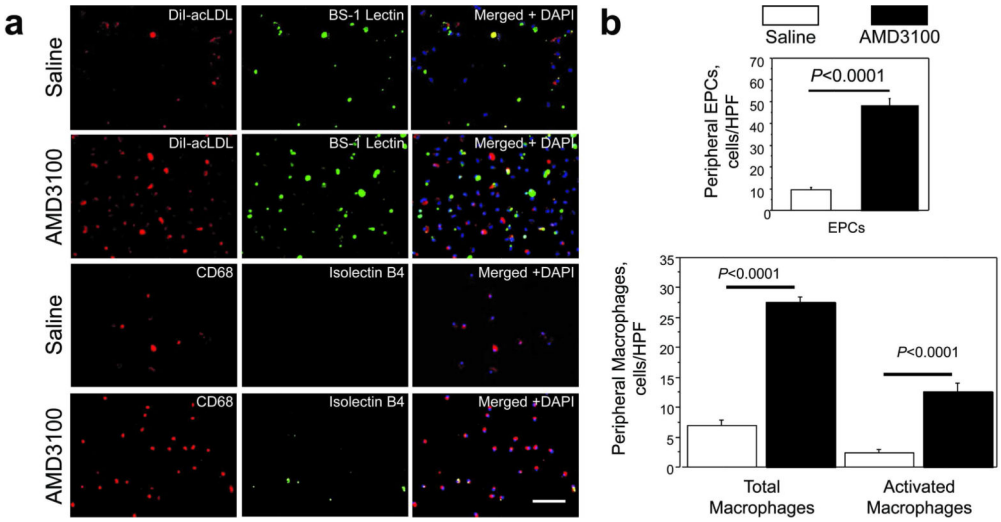

Figure 4. Mobilization of bone marrow–derived cells

The number of EPCs and macrophages in the peripheral blood was determined 7 days after wounds were treated with 6 mg/kg AMD3100 in 30 μL saline or saline alone. (**A**) Mononuclear cells were isolated from 500 μL of peripheral blood, then incubated with DiI-acLDL (red) and stained with FITC–conjugated BS1 lectin (green), or stained for the expression of CD68 (red) and isolectin B4 (green); nuclei were counterstained with DAPI (blue). Bar=100 μm. (**B**) EPC counts were quantified as the number of cells stained positively for both DiI-acLDL and BS-1 lectin, total macrophage counts were quantified as the number of cells stained positively for CD68, and activated macrophages were quantified as the number of cells stained positively for both CD68 and isolectin B4.

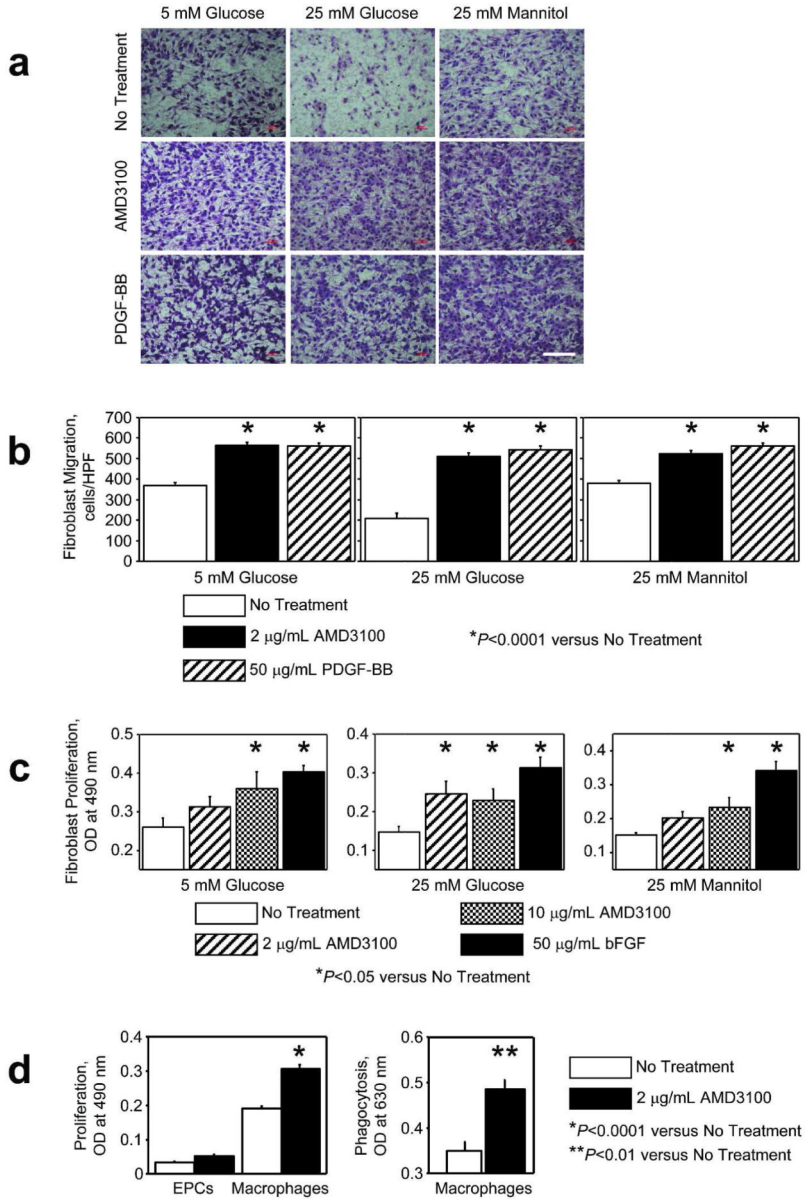

Figure 5. Activity of diabetic mouse fibroblasts, macrophages, and EPCs

(**A, B**) Fibroblast migration toward 0 μg/mL and 2 μg/mL AMD3100 or 50 μg/mL PDGF-BB (positive control) was evaluated via a modified Boyden's chamber assay in 5 mmol/L or 25 mmol/L D-glucose, or in 25 mmol/L D-mannitol to serve as an osmotic control for the high-glucose condition. Bar=100 μm. (**C**) Fibroblasts were treated with or without 2 μg/mL or 10 μg/mL AMD3100, or with 50 μg/mL basic fibroblast growth factor (bFGF, positive control), for 50 hours, and then fibroblast proliferation was evaluated via the CellTiter 96 nonradioactive cell proliferation assay in 5 mmol/L or 25 mmol/L D-glucose, or in 25 mmol/L D-mannitol to serve as an osmotic control for the high-glucose condition. (**D**) EPC proliferation, macrophage proliferation, and macrophage phagocytosis activity were assessed after treatment with or without 2 μg/mL AMD3100 for 50 (proliferation) or 24 (phagocytosis) hours; proliferation was assessed via the CellTiter 96 nonradioactive cell

proliferation assay, and phagocytosis was assessed via the CytoSelect™ 96-well phagocytosis assay (red blood cell, colorimetric format).

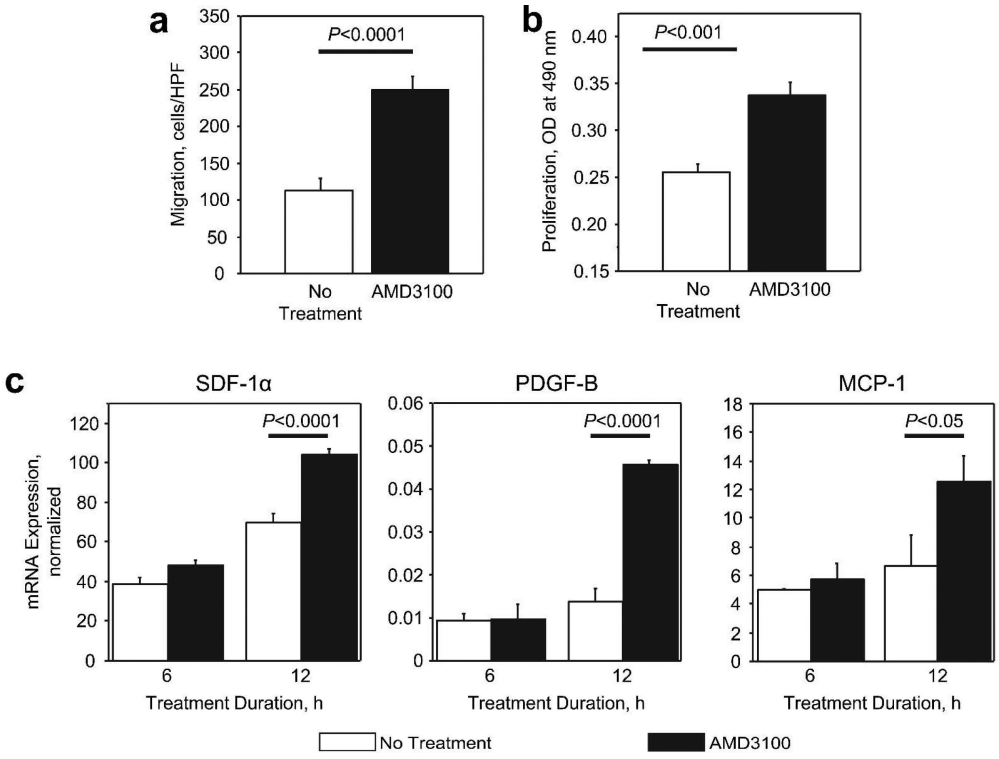

Figure 6. Activity and mRNA expression in 3T3 fibroblasts after treatment with AMD3100

(**A**) The migration of 3T3 fibroblasts toward 2 μg/mL AMD3100 was evaluated via a modified Boyden's chamber assay. (**B**) 3T3 fibroblasts were treated with or without 2 μg/mL AMD3100 for 48 hours, then proliferation was evaluated via the CellTiter 96 nonradioactive cell proliferation assay. (**C**) 3T3 fibroblasts were treated with or without 2 μg/mL AMD3100 for 6 or 12 hours; then, the mRNA expression of SDF-1α, PDGF-B, and monocyte chemotactic protein-1 (MCP-1) was assessed via quantitative real-time RT-PCR and normalized to 18S rRNA expression.